Effect of Nonpolar Substitutions of the Conserved Phe[11] in the Fusion Peptide of HIV-1 gp41 on Its Function, Structure, and Organization in Membranes[†]

Moshe Pritsker,[‡] Joseph Rucker,[§] Trevor L. Hoffman,[§] Robert W. Doms,[§] and Yechiel Shai*,[‡]

Department of Biological Chemistry, Weizmann Institute of Science, Rehovot 76100, Israel, and Department of Pathology and Laboratory Medicine, University of Pennsylvania, Philadelphia, Pennsylvania 19104

Received February 1, 1999; Revised Manuscript Received May 18, 1999

ABSTRACT: The fusion domain of the HIV-1 envelope glycoprotein (gp120−gp41) is a conserved hydrophobic region located at the N-terminus of the transmembrane subunit (gp41). A prominent feature of this domain is a conserved five-residue "FLGFL" sequence at positions 8−12. Mutation of the highly conserved Phe[11] to Val (F11V), presumed not to significantly affect the hydrophobicity and the structure of this region, has been shown to decrease the level of syncytium formation and virus infectivity. Here we show that the substitution of Gly for Phe[11] (F11G) reduces cell−cell fusion activity by 80−90%. To determine the effect of these mutations on the properties of the fusion peptide, a 33-residue peptide (WT) identical to the extended fusion domain and its F11V and F11G mutants were synthesized, fluorescently labeled, and studied with respect to their function, structure, and organization in phospholipid membranes. The WT peptide alone induced fusion of both zwitterionic (PC/Chol) and negatively charged (PS/PC/Chol and POPG) vesicles, in contrast to a 23-mer fusion peptide lacking the C-terminal domain which has been shown to be inactive with PC vesicles but able to induce fusion of POPG vesicles which had been preaggragated with Ca^{2+} or Mg^{2+}. The F11V peptide preserved 50% activity, and the F11G peptide was virtually inactive. ATR−FTIR spectroscopy indicated similar secondary structure of the peptides in multibilayers that was independent of membrane composition. Furthermore, all the peptides increased the extent of lipid disorder to a similar extent, but the kinetics of amide II H to D exchange was in the following order: F11G > F11V > WT. Fluorescence studies in the presence of membranes, as well as SDS−PAGE, revealed that the WT and F11V peptides self-associate to similar levels while F11G exhibited a decreased level of self-association. The data suggest that the FLGFL motif contributes to the functional organization of the HIV-1 fusion peptide and that the C-terminal domain following the fusion peptide contributes to the membrane fusion process.

Membrane fusion is an essential process for the infectious entry of enveloped viruses into host cells. The envelope glycoprotein gp160 of the human immunodeficiency virus type 1 (HIV-1) contains two noncovalently associated subunits, gp120 and gp41 (*1*), and mediates the membrane fusion activity of the virus. The outer surface subunit, gp120, contains sites necessary for viral binding to target cells containing CD4 (*2*) and chemokine receptors (*3*−*5*), whereas the transmembrane gp41 is responsible for the fusion process between viral and cell membranes (*6*). The binding of the gp120 subunit to the CD4 receptor induces a conformational change in the glycoprotein which enables it to interact with a chemokine receptor (*7*−*10*). This in turn is thought to result in the exposure of the previously hidden hydrophobic N-terminal domain of gp41, and its penetration into the target cell membrane. This hydrophobic domain, designated the "fusion peptide", is highly homologous with equivalent domains of other enveloped viruses (*11*). A prominent feature among the HIV family is the absolutely conserved, five-residue "FLGFL" sequence at positions 8−12. Interestingly, the "FXG" motif is also highly conserved in the fusion peptides of paramyxoviruses (*12*).

Evidence for the role of the fusion peptide domain in mediating membrane fusion comes from mutagenesis studies of intact envelope proteins, as well as from studies with synthetic fusion peptides and their analogues. Site-specific mutations in the fusion peptide domain of various viruses can decrease or increase their activity. For example, polar substitutions in the fusion peptides of HIV-1 (*13*) and SIV (*14*) can decrease the level of syncytium formation. Gly to Ala substitutions in the fusion peptide of SIV (*14*) and the paramixovirus SV5 (*15*), anticipated to enhance the overall hydrophobicity and α-helix formation, enhanced syncytium formation. On the other hand, mutation in the fusion peptide of HIV-1 of Gly at various positions to Val which enhances α-helix formation decreases the level of syncytium formation and virus infectivity (*16*). It should be noted that while mutations in other regions of envelope proteins can also decrease activity (*17*, *18*) only the fusion peptide is believed to be directly involved in the actual membrane fusion event. Durrer et al. (*19*), using a radiolabeled photoaffinity reagent, showed that during low pH-induced membrane insertion of influenza

[†] This work was supported in part by the Basic Research Foundation administered by the Israel Academy of Sciences and Humanities.

* To whom correspondence should be addressed: Department of Biological Chemistry, Weizmann Institute of Science, Rehovot 76100, Israel. Telephone: 972-8-9342711. Fax: 972-8-9344112. E-mail: bmshai@weizmann.weizmann.ac.il.

[‡] Weizmann Institute of Science.

[§] University of Pennsylvania.

10.1021/bi990232e CCC: $18.00
Published on Web 08/10/1999

virus hemagglutinin, the only part of the protein that inserts into the membrane is the N-terminal fusion peptide.

To study the mechanisms by which fusion peptide mutations modulate virus−cell fusion, extensive structural and functional studies with synthetic peptides corresponding to fusion peptides derived from a number of viruses have been performed (*20*−*32*). In most cases, a correlation was found between the function of the fusion peptides and the activity of the intact proteins. However, in the case of the HIV-1 fusion peptide, structure and function were shown to be dependent on the length of the fusion peptide. For example, the effect of mutation of Val at position 2 to Glu has been studied with 23 (*33*)- and 33-residue (*31*) fusion peptides and their V2E mutants. In both studies, the mutants lacked fusogenic activity. However, the 22-mer and the 33-mer exhibited several differences. The 33-mer V2E but not the 23-mer peptide could inhibit fusion of model membranes induced by the wild-type fusion peptide, as well as fusion of cells expressing gp41 with cells expressing the CD4 receptor (*31*). Furthermore, the results of similar CD[1] and FTIR studies with the synthetic 23-mer and shorter fusion peptides of HIV and SIV depict a more complex picture (*25*, *28*, *30*, *33*−*36*). In these cases, differing proportions of α-helix and *β*-sheet conformations are observed depending on environmental conditions. For example, Rafalski et al. (*28*) found that with negatively charged vesicles, the HIV fusion peptide binds in an α-helical conformation and induces fusion, whereas with neutral liposomes, the bound peptide adopts a *β*-structure and does not induce fusion. In contrast, also using negatively charged vesicles, Nieva et al. (*35*) concluded that membrane-bound α-helical conformations are associated with leakage, while *β*-sheet conformations are associated with fusion. Nevertheless, neither one of the shorter versions could induce fusion of PC membranes if they do not include PE (*37*) which promotes the fusion process (*38*). The outer surface of normal cells is composed of predominantly zwitterionic phospholipids (PC). Therefore, the inability of fusion peptides to induce fusion of membranes independent of their charge may present a better correlation between model and biological studies.

In this study, we investigated the effect of mutation of the highly conserved Phe[11] of the HIV-1 fusion peptide on the activity of intact gp41 and on the function and properties of synthetic 33-residue fusion peptides. The F11V substitution reduced fusogenic activity as previously reported (*16*), even though introduction of Val instead of Phe was expected to change significantly neither the hydrophobicity nor the secondary structure of the fusion peptide. The second mutation F11G, introduced in this study in gp41 and in the synthetic fusion peptide, was expected to reduce the bulkiness of this region as well as the α-helicity of the fusion peptide, as there are other two glycines nearby, namely, Gly[10] and Gly[13]. The peptides were investigated for their function, structure, and interaction with phospholipid membranes. CD and ATR−FTIR spectroscopy were used to determine the structure and orientation of the peptides in phospholipid membranes. The peptides were also labeled with fluorescent probes to facilitate determination of their ability to bind and oligomerize in phospholipid membranes. The results are discussed in line with several properties which are affected by the Phe[11] mutation, and the importance of the C-terminal domain of the fusion peptide is assisting in membrane fusion.

[1] Abbreviations: ATR−FTIR, attenuated total reflectance−Fourier transform infrared; Boc, butyloxycarbonyl; CD, circular dichroism; LUV, large unilamellar vesicles; NBD-F, 4-fluoro-7-nitrobenz-2-oxa-1,3-diazole; Pam, phenylacetamidomethyl; PC, egg phosphatidylcholine; POPG, L-α-phosphatidyl-DL-glycerol, *β*-oleyl-*γ*-palmitoyl; PS, phosphatidylserine; PBS, phosphate-buffered saline (pH 7.3); RP-HPLC, reverse phase high-performance liquid chromatography; Rho, tetramethylrhodamine; SUV, small unilamellar vesicles; TFA, trifluoroacetic acid.

MATERIALS AND METHODS

Materials. BOC-amino acid phenylacetamidomethyl (PAM)-resin was purchased from Applied Biosystems (Foster City, CA), and BOC-amino acids were obtained from Bachem. NBD-fluoride, L-α-phosphatidyl-DL-glycerol, *β*-oleyl-*γ*-palmitoyl (POPG), and the reagents for peptide synthesis were obtained from Sigma. Egg phosphatidylcholine (PC) and phosphatidylserine (PS) from bovine spinal cord (sodium salt grade I) were purchased from Lipid Products (South Nutfield, U.K.). Cholesterol (extra pure), purchased from Merck (Darmstadt, Germany), was recrystallized twice from ethanol. *N*-[Lissamine rhodamine B-sulfonyl]dioleoylphosphatidylethanolamine (Rho-PE), *N*-(7-nitrobenz-2-oxa-1,3-diazol-4-yl)dioleoylphosphatidylethanolamine (NBD-PE) and 5(6)-carboxytetramethylrhodamine (Rho) were purchased from Molecular Probes (Junction City, OR). Triton X-100, reduced form, was purchased from Aldrich. All other reagents were analytical grade. Buffers were prepared using double-glass-distilled water. Phosphate-buffered saline (PBS) was composed of NaCl (8 gm/L), KCl (0.2 gm/L), KH_2PO_4 (0.2 gm/L), and Na_2HPO_4 (1.09 gm/L) (pH 7.4).

Plasmids and Cells. BH8 envelope glycoprotein (*5*) was expressed using the T7 promoter in the plasmid pSP73. The F11G substitution was engineered using the Quickchange Site-Directed Mutagenesis Kit (Stratagene) and confirmed by DNA sequencing. vTF1.1 was used to express T7 RNA polymerase off of the vaccinia late promoter (*39*, *40*). CXCR4 was expressed under the control of the CMV promoter in the plasmid pCDNA3 (Invitrogen). A plasmid containing the luciferase gene under the control of the T7 promoter (T7-luc) was from Promega. QT6 and 293T cells were maintained in DMEM supplemented with 10% fetal bovine serum (FBS).

Peptide Synthesis, Fluorescent Labeling, and Purification of Peptides. The peptides were synthesized by a solid phase method on PAM-amino acid resin (0.15 molar equiv) (*41*−*43*). Labeling of the N-terminus of the peptides was achieved as previously described (*44*, *45*). Briefly, resin-bound peptides, with their amino acid side chains fully protected, were treated with trifluoroacetic acid (TFA) so the BOC protecting group could be removed from their N-terminal amino groups, while keeping all the other reactive amine groups of the attached peptides protected. The resin-bound peptides were then reacted with the desired fluorescent probe, and finally cleaved from the resins by HF, extracted with TFA, and precipitated with ether. This procedure yielded peptides selectively labeled with fluorescent probes at their N-terminal amino acid. The synthetic peptides were purified (>95% homogeneity) on a C4 reversed phase Bio-Rad analytical column (250 mm × 4.2 mm, 300 Å pore size, 5 *μ*M particle size) using a linear gradient of 25 to 80% acetonitrile in

0.05% TFA, over the course of 40 min. The peptides were subjected to amino acid analysis so their composition could be confirmed.

Preparation of Lipid Vesicles. Small unilamellar vesicles (SUV) were prepared by sonication from PC/PS/Chol (4:4:1 w/w), PC/Chol (10:1 w/w), or POPG. Large unilamellar vesicles (LUV) were also prepared from the same lipid compositions by extrusion through polycarbonate membranes (*46*), and when necessary with 0.6 mol % Rho-PE and NBD-PE. The procedure was as follows. Dry lipids were hydrated in buffer and dispersed by vortexing to produce large multilamellar vesicles. The lipid suspension was subjected to five freeze−thaw cycles and then extruded eight times through a polycarbonate membrane with 0.1 or 0.4 μm diameter pores (Nuclepore Corp., Pleasanton, CA).

Peptide-Induced Lipid Mixing. The level of lipid mixing of LUV was measured using a fluorescence probe dilution assay, based on resonance energy transfer measurements (*47*). LUV composed of PC/PS/Chol (4:4:1 w/w), PC/Chol (10:1 w/w), or POPG, containing 0.6 mol % NBD-PE (energy donor) and 0.6 mol % Rho-PE (energy acceptor), were prepared in PBS. A mixture of labeled and unlabeled LUV (1:4) was suspended in 400 μL of PBS at room temperature, and a small volume of peptide in DMSO was added. The increase in NBD fluorescence at 530 nm was monitored with the excitation wavelength set at 467 nm. The inner-filter effect was minimized by using a 0.5 cm path length cuvette. The fluorescence intensity before the addition of the peptide was termed 0% lipid mixing, and the fluorescence intensity upon the addition of reduced (to eliminate quenching of the NBD probe) Triton X-100 (0.25% v/v) was termed 100% lipid mixing. All the fluorescence measurements were taken on a Perkin-Elmer LS-50B spectroflourimeter.

Visualization of Vesicle Fusion by Electron Microscopy. The effects of the peptides on liposomal suspensions were examined by negative staining electron microscopy. A drop containing LUV alone or a mixture of LUV and a peptide was deposited onto a carbon-coated grid and negatively stained with 2% uranyl acetate. The grids were examined using a JEOL JEM 100B electron microscope (Japan Electron Optics Laboratory Co., Tokyo, Japan).

Visible Absorbance Measurements. The changes in the size of the vesicles were measured by visible absorbance measurements. Aliquots of peptide stock solutions were added to 200 μL suspensions of 90 μM LUV (4:4:1) in PBS. Absorbance was measured at 405 nm using Bio-Tek Instruments microplate reader before and after the addition of peptide.

Binding of the Peptides to the Membrane and Localization of the NBD Probe. The ability of the peptides to bind phospholipid membranes was evaluated by using NBD-labeled peptides. NBD-labeled peptide (final concentration of 0.1 μM) was added to 2 mL of PBS, with and without SUV (400 μM). The time profiles were recorded with excitation set at 467 nm (10 mm slit width) and emission set at 530 nm (8 mm slit width). After the establishment of a constant fluorescence intensity, the emission spectra were recorded under the same conditions. In these experiments, the lipid:peptide molar ratio was elevated (4000:1) such that most of the peptides are assumed to be bound to the vesicles.

The degree of peptide association with lipid vesicles was measured by adding 0.1 μM NBD-labeled peptide to 2 mL of PBS solution in the presence of SUV at different concentrations. The fluorescence intensity was measured in the time-dependent mode, with excitation set at 467 nm (10 mm slit midth) and emission set at 530 nm (8 mm slit width), until a maximal intensity was achieved. A separate experiment was carried out for each vesicle concentration. The fluorescence values, F, were corrected by subtracting the corresponding blank (buffer with the same amount of vesicles). The increases in the fluorescence intensity, $F - F_0$, where F_0 is the fluorescence intensity in the absence of SUV, were plotted as a function of the lipid:peptide molar ratio.

Accessibility of the Peptides to Proteolytic Cleavage in the Membrane-Bound State. NBD fluorescence is sensitive to its environment (*44*, *48*). The fluorescence quantum yield is low in solution and high in the membrane-bound state. NBD-labeled peptide (0.1 μM) was added to 2 mL of PBS solution containing SUV (400 μM) concomitant with an increase in the fluorescence intensity. The proteolytic enzyme proteinase K (100 μg) was then added, and the fluorescence intensity was monitored at 530 nm (8 mm slit width) with the excitation set at 467 nm (10 mm slit width). Cleavage of membrane-bound NBD-labeled peptide would release the NBD-labeled fragment into the solution and hence will reduce the fluorescence intensity. In a control experiment, the enzyme was added first to the solution containing the labeled peptide, followed by the addition of SUV. The emission at the end of the control experiment was termed 100%.

Attenuated Total Reflectance−Fourier Transform Infrared (ATR−FTIR) Spectroscopy. Spectra were obtained with a Bruker Equinox55 FTIR spectrometer coupled with an ATR device. For each spectrum, 60 scans were collected, with a resolution of 4 cm^{-1}. The preparation of the samples was as follows. Lipid/peptide mixtures were prepared by dissolving them together in a 1:2 MeOH/CH_2Cl_2 mixture. A mixture of phospholipids alone or with a peptide was deposited on a Zn−Se prism and dried under vacuum. Spectra were recorded, and the respective pure phospholipid was subtracted to yield the difference spectra to determine the amide I absorption peaks of the peptides. For each spectrum, the background was that of a clean prism under the same experimental conditions. To wet the samples, the dry lipid/peptide films were exposed to D_2O vapor. Spectra were measured after equilibration.

The spectra were analyzed as previously reported (*49*). Curve fitting of the amide 1 band area (1600−1700 cm^{-1}), assuming Voight line shapes for the IR peaks, was performed to determine the relative contents of the different secondary structure elements.

ATR−FTIR Data Analysis. The ATR electric fields of incident light were calculated by using the following formulas (*50*, *51*):

$$E_x = \frac{2\cos\theta\sqrt{\sin^2\theta - {n_{21}}^2}}{\sqrt{(1-{n_{21}}^2)[(1+{n_{21}}^2)\sin^2\theta - {n_{21}}^2]}}$$

$$E_y = \frac{2\cos\theta}{\sqrt{1-{n_{21}}^2}}$$

$$E_z = \frac{2\sin\theta\cos\theta}{\sqrt{(1-{n_{21}}^2)[(1+{n_{21}}^2)\sin^2\theta - {n_{21}}^2]}}$$

where θ is the angle of a light beam to the prism normal at the point of reflection (45°) and $n_{21} = n_2/n_1$ [n_1 and n_2 are the refractive indices of Zn−Se (taken to be 2.4) and the membrane sample (taken to be 1.5), respectively]. Under these conditions, E_x, E_y, and E_z are 1.40, 1.52, and 1.64, respectively. The electric field components together with the dichroic ratio [defined as the ratio between absorption of parallel (to a membrane plane), A_p, and perpendicular polarized incident light, A_s] are used to calculate the orientation order parameter, f, with the following formula:

$$R^{ATR} = \frac{A_p}{A_s} = \frac{E_x^2}{E_y^2} + \frac{\frac{E_z^2}{E_y^2}\left(f\cos^2\alpha + \frac{1-f}{3}\right)}{\frac{f\sin^2\alpha}{2} + \frac{1-f}{3}}$$

where α is the angle between the transition moment of the CH_2 asymmetric vibration (~2922 cm^{-1}) and the helix axis. Lipid order parameters were obtained from the symmetric (~2853 cm^{-1}) and asymmetric (~2922 cm^{-1}) lipid stretching mode setting α of 90° (*51*). The orientation order parameter, f, allows us to calculate the average angle of the lipid chains relative to the membrane normal, γ, with the following formula:

$$f = \frac{3\cos^2\gamma - 1}{2}$$

Rhodamine Fluorescence Experiment. Rhodamine fluorescence is highly sensitive to self-quenching but poorly affected by the dielectric constant of its environment. Therefore, the tendency of the peptides to oligomerize in solution and in the membrane was tested utilizing Rho-labeled peptides. Changes in the fluorescence were measured following the addition of a Rho-labeled peptide (final concentration of 0.025−0.5 μM) to 2 mL of PBS in the presence or absence of SUV (final concentration of 400 μM). In this range of concentrations, most of the peptide is bound to the vesicles (see the section on peptide binding to membranes). Excitation was set at 530 nm (10 cm slit width) and emission at 587 nm (8 cm slit width).

Determination of the Oligomeric States of the Peptides by SDS−PAGE. The experiments were carried out as described in ref *52*. Peptides were dissolved by sonication in a sample solubilization buffer composed of 2% SDS, 0.065 M Tris-HCl (pH 6.8), and 10% glycerol. Fixing, staining, and destaining times were shortened to 1 min, 1 h, and overnight, respectively, to decrease the magnitude of diffusion effects.

RESULTS

Reporter Gene Assay for Cell−Cell Fusion

Previous studies have shown that the F11V mutation in gp41 adversely affects viral membrane fusion. To evaluate the consequences of a Gly substitution at this position, we compared the ability of wild-type Env and F11G Env to mediate cell−cell fusion (*40*, *53*). Briefly, 293T effector cells were infected with a vaccinia virus encoding T7 RNA polymerase and then transfected with plasmids bearing the *env* genes under the control of the T7 promoter. Target cells were prepared by transient transfection of QT6 cells with plasmids encoding CD4, either pCDNA3 or pCDNA3-CXCR4, and with T7-luc. After overnight expression, effector and target cells were mixed and allowed to fuse for 2−8 h. Cells expressing wild-type Env and the F11G mutant were lysed, and aliquots were subjected to SDS−PAGE and Western blotting to assess the efficiency with which gp160 was cleaved to gp120 and gp41 subunits. Cytoplasmic mixing of effector cells with target cells leads to expression of luciferase which can be easily quantitated using a luminometer. Figure 1 shows that F11G mediated fusion at levels that were <10% of that of the wild type. The F11G Env was, however, expressed and processed (i.e., cleaved into gp120 and gp41 subunits) as efficiently as the wild-type protein. Thus, we conclude that the F11G mutation specifically affects the ability of HIV-1 Env to mediate membrane fusion.

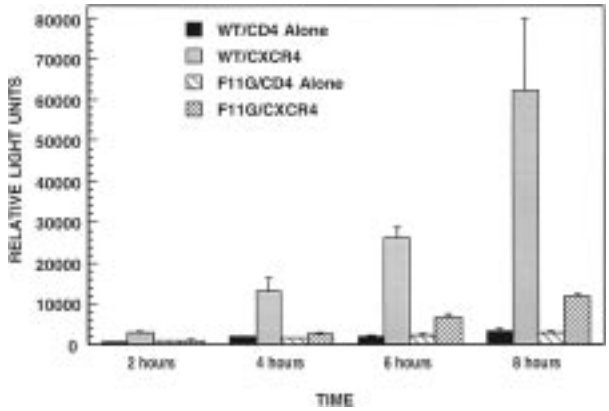

FIGURE 1: Cell−cell reporter gene fusion assay. 293T effector cells and QT6 target cells (with plasmids encoding CD4, either pCDNA3 or pCDNA3-CXCR4, and with T7-luc) were mixed and allowed to fuse for 2−8 h. Cytoplasmic mixing of effector cells with target cells leads to expression of luciferase which was quantitated using a luminometer. The figure shows the time dependence of the fusion process.

Studies with the Fusion Peptides

Peptides representing the 33 N-terminal amino acid residues of gp41 (LAV1a) and its F11V and F11G mutants were synthesized and fluorescently labeled at their N-terminal amino acids with either NBD (to serve in the binding experiments) or rhodamine (to serve in homo energy transfer). The sequences of the peptides and their designations are given in Table 1.

Functional Properties of the Peptides

Reduced Ability of the Mutants To Induce Lipid Mixing of both Zwitterionic and Negatively Charged Vesicles. The induction of intervesicular lipid mixing by the peptides as a measure of their fusogenic activity was tested with PC/PS/Chol (4:4:1 w/w), PC/Chol (10:1), or POPG LUV utilizing the probe dilution assay as described by Struck et al. (*47*). In separate experiments, increasing amounts of each peptide were added to a fixed amount of vesicles. To compare the activity of the three peptides, the maximal values of the fluorescence intensity, reached after the addition of the peptides, were plotted as a function of the peptide:lipid molar ratio. Figure 2 shows the dose−response curves with PC/PS/Chol (panel A) and PC/Chol (panel B) LUV. The results

Table 1: Amino Acid Sequences of the Peptides and Their Fluorescently Labeled Analogues

No.	Peptide Designation		Sequence[a]
1	WT	X=H	X-HN- A V G I G A L F L G F L G A A G S T M G A R S M T L T V Q A R Q L - COOH
2	NBD-WT	X=NBD	
3	Rho-WT	X=Rho	
4	F11V	X=H	X-HN- A V G I G A L F L G **V** L G A A G S T M G A R S M T L T V Q A R Q L - COOH
5	NBD-F11V	X=NBD	
6	Rho-F11V	X=NBD	
7	F11G	X=H	X-HN- A V G I G A L F L G **G** L G A A G S T M G A R S M T L T V Q A R Q L - COOH
8	NBD-F11G	X=NBD	
9	Rho-F11G	X=NBD	

[a] Substituted amino acids are underlined and bold.

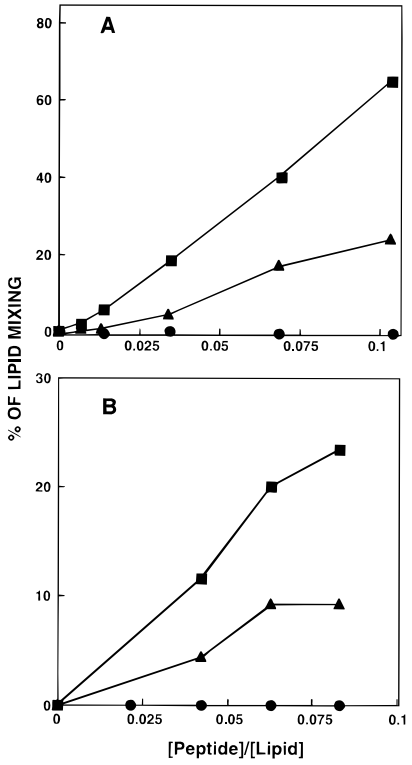

FIGURE 2: Dose dependence of lipid mixing of PC/PS/Chol (4:4:1) (A) and PC/Chol (9:1) (B) LUV induced by the peptides. Peptide aliquots were added to mixtures of LUV (22 μM phospholipid concentration) containing 0.6 mol % NBD-PE and 0.6 mol % Rho-PE and unlabeled LUV (88 μM phospholipid concentration) in PBS. The maximal values of the NBD-PE fluorescence intensity, reached after the addition of the peptides, were plotted as a function of the peptide:lipid molar ratio. The fluorescence intensity upon the addition of Triton X-100 (0.25% v/v) was termed 100%: (■) wild type, (▲) F11V, and (●) F11G.

with POPG were similar to those obtained with PS/PC, but F11G had only slight activity (~5%) at the highest peptide:lipid molar ratio that was tested (data not shown). The data reveal that the fusion peptide can induce lipid mixing of both zwitterionic and negatively charged phospholipid membranes, without the need for secondary cations. This is different from what has been found with shorter versions of the fusion peptides (that do not include the 10 amino acids at the C-terminal side) which did not induce fusion of PC vesicles (*28*) and required Ca^{2+} or Mg^{2+} to cause fusion of negatively charged membranes (*35*). We have also examined the 16-mer N-terminal fusion peptide (*37*) which was inactive with PC vesicles and had a 5-fold reduced activity compared to that of the wild-type peptide with the negatively charged vesicles. However, in the presence of Mg^{2+}, the peptide retained 60% of the activity of the wild type (data not shown). The activity with PS/PC/Chol was twice that observed with PC/Chol vesicles at the same peptide:lipid molar ratio, perhaps the result of a slightly higher level of partitioning of the peptides within negatively charged than within zwitterionic membranes. The data also revealed that F11V has a reduced ability to induce lipid mixing compared to the wild type, whereas F11G was practically inactive. This tendency was found also with the intact gp41 compared to its F11V (*16*) and F11G mutants (Figure 1). The fusogenic activity of the fluorescently labeled peptides could not be studied in this assay but was tested by visualization using electron microscopy (see the next section).

Membrane Fusion Visualized by Electron Microscopy. To confirm that the intervesicular lipid mixing was the result of membrane fusion, electron microscopy was used. LUV (90 μM) were visualized by negative stain electron microscopy before and after addition of peptides (5 μM). Figure 3 shows representative micrographs of PC/PS/Chol (4:4:1) LUV taken at pH 7.3 without peptide (panel A), with the wild-type peptide (panel B), with the F11V peptide (panel C), and with the F11G peptide (panel D). The micrographs demonstrate that the lipid mixing observed with the wild-type peptide was associated with an increase in vesicle size, whereas with F11V this occurred to a lesser extent. Such size increases were not observed with the F11G mutant. When fluorescently labeled peptides were used, the morphology changes were similar to those obtained with unlabeled peptides (data not shown).

F11G Has a Reduced Ability To Induce Vesicle Aggregation, whereas Wild-Type and F11V Have Similar Activities. Previous studies with shorter versions of fusion peptides revealed that aggregation of negatively charged vesicles is

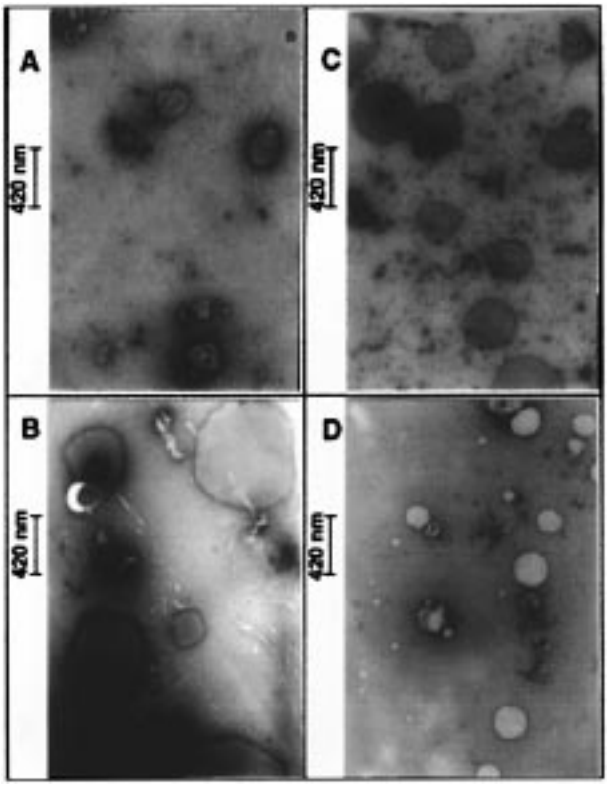

FIGURE 3: Electron micrographs of negatively stained liposomes. (A) PC/PS/Chol (4:4:1) LUV (110 μM) alone, (B) PC/PS/Chol (4:4:1) LUV incubated with 5 μM wild-type peptide for 15 min, (C) PC/PS/Chol (4:4:1) LUV incubated with 5 μM F11V peptide for 15 min, and (D) PC/PS/Chol (4:4:1) LUV incubated with 5 μM F11G.

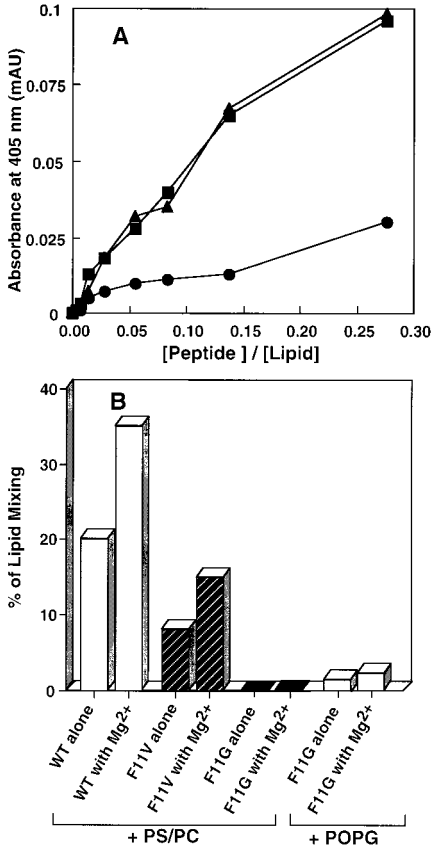

FIGURE 4: (A) Detection of aggregation and/or fusion by observing absorbance changes at 405 nm of liposomes mixed with peptides. The peptides were added to 110 μM PC/PS/Chol (4:4:1) LUV in PBS. The changes in absorbance at 405 nm are plotted vs the peptide:lipid molar ratio. Activities of the wild type and F11V with POPG were similar to those with PS/PC and therefore are not given: (■) wild type, (▲) F11V, and (●) F11G. (B) Effect of Mg^{2+} on lipid mixing induced by the peptides. A mixture of PC/PS/Chol (4:4:1) or POPG LUV was incubated, alone or with Mg^{2+}, for 5 min. Peptides were then added at a peptide:lipid molar ratio of 0.035. The increase in fluorescence intensity of NBD-PE was measured, and the percentage of maximum fusion is plotted.

an essential step in allowing their fusion (*35*). The ability of the peptides to induce vesicle aggregation was tested to investigate whether this property is responsible for the differences in their ability to cause membrane fusion. Changes in vesicle size distribution resulting from peptide-induced aggregation and/or fusion can be monitored by following the absorbance of the liposome suspension. The changes in absorbance at 405 nm as a function of the peptide:lipid molar ratio are shown in Figure 4A. The data reveal that at both fusion and subfusion concentrations that were tested, the wild type and F11V possess equal abilities to aggregate vesicles, whereas F11G has reduced activity.

Lipid Mixing Induced by the Peptides after Preaggregation with Mg^{2+}. Previous studies demonstrated that a shorter version of the HIV-1 fusion peptide which does not include the 10-amino acid extended hydrophilic region can cause fusion of negatively charged membranes only in the presence of secondary ions (*28*). We therefore examined the potential of the peptides to induce fusion of preaggregated PS/PC/Chol and POPG vesicles, as previously described (*35*). Figure 4B shows the results following addition of the peptides to LUV at a lipid:peptide molar ratio of 0.034 before and after their preincubation in a medium containing 5 mM Mg^{2+}. The results obtained for the wild type and F11V were similar whether PS/PC or POPG was used, and therefore, only results with PS/PC/Chol are given. At these concentrations, Mg^{2+} is known to cause aggregation but not fusion of PS LUV (*54*−*56*). A comparison of the results in the absence or presence of Mg^{2+} shows that PS/PC/Chol vesicle preaggregation enhances fusion only with the wild type and F11V, but no fusion was detected with the F11G mutant. However, slight activity was obtained with F11G in POPG (Figure 4B, two right columns).

Organization of the Peptides in Membranes

Binding of the Peptides to Phospholipid Membranes. The fluorescence emission intensity of the NBD-labeled peptides was monitored in PBS before and after addition of SUV. In buffer, the peptides (0.1 μM) exhibited emission spectra similar to that of the NBD moiety dissolved in water (*44*, *48*), with low intensity and a maximum at ~545 nm (Figure 5). However, upon addition of the peptides to a buffer solution containing SUV (400 μM), the fluorescence emission intensities increased concomitant with blue shifts of the emission maxima to 519 ± 1 nm for both the wild type and F11V, and 523 ± 1 nm for F11G (Figure 5). An increase in fluorescence and blue shifts reflects binding of surface-active NBD-labeled peptides to phospholipid membranes (*44*, *57*) and is consistent with the NBD probe located within the hydrophobic core of the membrane (*48*). However, we cannot rule out some effect on the fluorescence due to different aggregation states for the peptides in the membrane. The time profiles of the fluorescence changes at 530 nm show

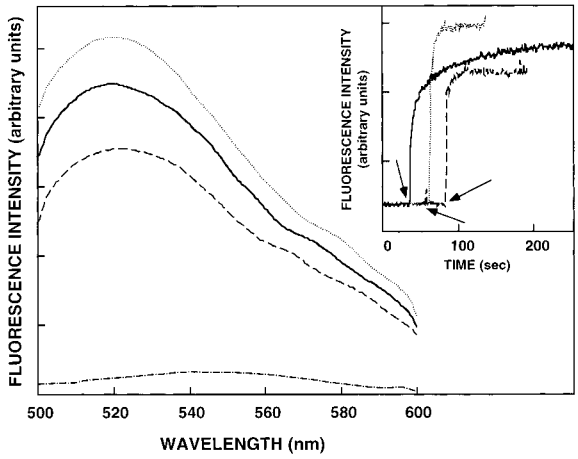

FIGURE 5: Fluorescence emission spectra of the NBD-labeled peptides (0.1 μM) in buffer or in the presence of PC/PS/Chol (4:4:1) SUV (400 μM). The excitation wavelength was set at 467 nm, and emission was scanned from 500 to 600 nm: (— · —) wild type in buffer, (—) wild type in the presence of SUV, (•••) F11V in the presence of SUV, and (- - -) F11G in the presence of SUV. The emission spectra of F11V and F11G in buffer are similar to that of the wild type and therefore are not shown. (Inset) Kinetics of the increase in fluorescence intensity of the NBD-labeled peptides, when added to vesicle suspension. Designations are the same as in the main figure. Arrows denote the addition of peptides.

faster binding kinetics for F11G and F11V than for the wild type (inset of Figure 5). As will be shown, the wild-type peptide is in a higher aggregation state in solution than F11V and F11G, but is in an aggregation state in membranes similar to that of F11V. Therefore, upon binding to membranes, the wild-type peptide should dissociate to smaller oligomers. The slow kinetics of fluorescence increase observed for the wild type in the presence of membranes may be, therefore, due to dequenching of NBD fluorescence upon dissociation of WT to its smaller oligomers. In these experiments, the lipid:peptide molar ratio was consistently high so that spectral contributions of free peptides and bilayer disruption could be considered negligible.

The increases in the fluorescence intensity of the NBD-labeled peptides due to membrane partition were recorded as a function of the lipid:peptide molar ratios and are plotted in panels A and B of Figure 6 for PS/PC and PC vesicles, respectively. Such curves have been analyzed previously in evaluating the partition constant of binding (*58*). Since the peptides aggregate in the aqueous solution, their binding isotherms were not analyzed further. The shapes of the binding curves of the wild-type and F11V peptides are practically the same in both types of phospholipid membranes, and they become saturated at lipid:peptide molar ratios similar to those observed with the NBD-labeled antibacterial peptides DS-b (*44*, *59*), suggesting a partition coefficient on the order of 10^4 M^{-1} for both of them. However, F11G saturates at a higher lipid:peptide molar ratio which suggests a slightly lower level of partitioning into membranes compared to the wild type and F11V.

Susceptibility of Membrane-Bound Peptides to Proteolytic Cleavage. The susceptibility of membrane-bound NBD-WT, NBD-F11V, and NBD-F11G to proteolytic digestion by proteinase K was used as a method of determining whether the peptides are deeply inserted within the lipidic core of the membrane or were exposed to the solution. NBD-labeled

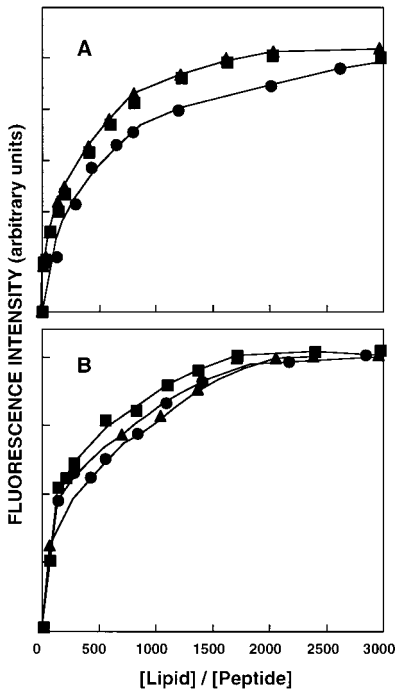

FIGURE 6: Increase in the fluorescence of NBD-labeled peptides (0.1 μM) when added to buffer in the presence of PC/PS/Chol (4:4:1) (A) or PC (B) SUV. Binding curves with POPG overlap those with PC/PS/Chol and therefore are not given. The measurements were performed with excitation set at 467 nm and emission monitored at 530 nm: (—) wild type, (▲) F11V, and (●) F11G.

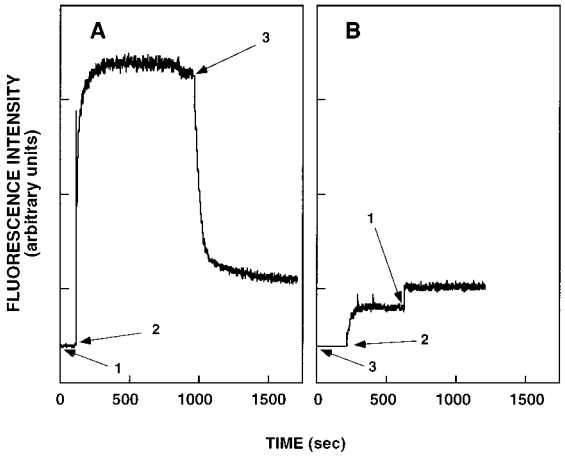

FIGURE 7: (A) Proteolytic digestion of membrane-bound NBD-labeled peptides. (B) Control experiment. The fluorescence emission spectra of NBD-labeled peptides were monitored at 530 nm with the excitation set at 467 nm: (1) addition of 400 μM SUV, (2) addition of 0.1 μM NBD-labeled F11G, and (3) addition of 100 μg of proteinase K.

peptides were treated with the proteolytic enzyme proteinase K before and after binding to phospholipid membranes. Figure 7A depicts an example of one such experimental profile for the F11G mutant using PS/PC vesicles. Similar results were obtained with PC and POPG vesicles and therefore are not shown. Vesicles were first added to PBS (time point 1), followed by the addition of NBD-labeled peptide (time point 2), which caused a large increase in fluorescence. Once the curve reached a plateau, indicating the completion of binding of NBD-F11G to the membrane, proteinase K was added (time point 3). Figure 7A shows

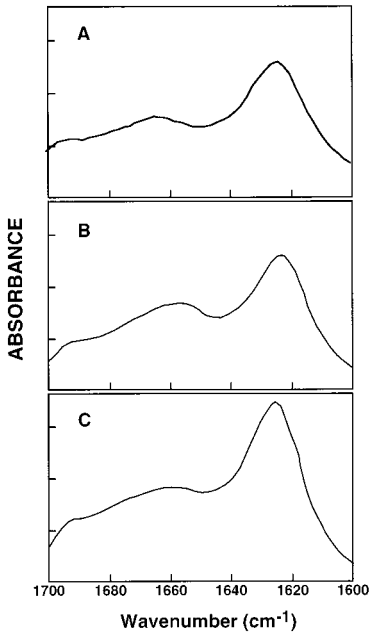

FIGURE 8: Attenuated total reflectance−Fourier transform infrared (ATR−FTIR) spectra of the amide I region of the peptides in PC multibilayers. Similar spectra were obtained in POPG and therefore are not given: (A) wild type, (B) F11V, and (C) F11G. The samples were prepared as described in Materials and Methods; the peptide: lipid molar ratio was 1:80. The spectra were analyzed using the curve fitting of the amide I band area assuming Voight line shapes for the IR peaks.

that following proteinase K treatment, the fluorescence of NBD-F11G decreased very fast, demonstrating release of the probe from the hydrophobic environment of the vesicles. This indicates that the labeled peptide is exposed to the aqueous phase and is susceptible to degradation in its membrane-bound state. Similar results were obtained with NBD-WT and NBD-F11V, but with slightly slower kinetics (data not shown). These data are in contrast with what has been found with lytic peptides which are inserted into the lipidic core of the membrane, and are therefore totally resistant to proteolytic digestion (*57*, *60*). The data also suggest that major portions of both the wild type and the two mutants are located on the surface of the vesicles and therefore are accessible to proteinase K. Control experiments were performed by adding NBD-labeled peptides to proteinase K prior to the addition of vesicles. When vesicles were added to a degraded peptide (time point 2 of Figure 7B), a small increase in fluorescence was observed, probably due to the binding of partially uncleaved peptides to vesicles.

Secondary Structure of the Peptides Determined by FTIR Spectroscopy. The secondary structure of the peptides was determined in zwitterionic PC and negatively charged POPG multibilayer lipid systems by using FTIR spectroscopy. Similar results were obtained whether PC or POPG lipids were used, and therefore, only data with PC are presented. The contributions of the various secondary structure elements to the amide I peak were obtained by curve fitting, using the values from Jackson et al. (*61*) (Figure 8). The main peak located at 1622−1626 cm^{-1} represents β-sheet structure. The second main peak at 1658 cm^{-1} could represent α-helix or disordered structure. The contributions of the other elements are relatively small. To distinguish between these two elements, the films containing the peptides were wetted by exposure to D_2O vapors. The peak area at 1658 cm^{-1} decreased due to fast H−D exchange of the amide protons. The results obtained with both dry and wet samples are summarized in Table 2. The major structure for all the peptides is β-sheet. We also followed changes in amide II absorption which represents mostly the N−H vibrational mode and, therefore, is more sensitive to proton exchange. The hydration caused a strong decrease in the amide II peak area at ∼1510−1590 cm^{-1} (N−H vibration) and appearance of the peak at ∼1410−1490 cm^{-1} (N−D vibration). The kinetics of exchange was followed, and spectra obtained after 15 min are shown in Figure 9. The data reveal that the kinetics of amide II exchange increase in the following order: F11G > F11V > wild type; this suggests that the N−H bond is more protected in the wild type than in the other two mutants. This may indicate that the stability of the secondary structure of the peptides in the membrane is in the following order: wild type > F11V > F11G.

Orientation of the Lipid Multibilayers and the Effect of the Peptides on Lipid Acyl Chain Order. The symmetric (ν_{sym} ∼ 2850 cm^{-1}) and antisymmetric ($\nu_{antisym}$ ∼ 2920 cm^{-1}) vibrations of the lipid methylene C−H bond are perpendicular to the molecular axis of a fully extended hydrocarbon chain. Thus, measurements of the infrared absorbance dichroism show the order and the orientation of the lipid sample relative to the prism surface. The *R* values for the lipid and lipid/peptide samples were calculated from the stronger $\nu_{antisym}(CH_2)$ peaks (Figure 10). The results are summarized in Table 3. The observed band position for $\nu_{antisym}(CH_2)$ at 2923 cm^{-1} indicates that the samples were in a liquid crystalline phase which is typical for biological membranes (*62*). The data show that the lipid samples were well ordered, thus confirming the validity of the determination of the peptide orientation. The peptides do not induce a significant change in the ordering of acyl chains (Table 3, graphs not shown). Similar results were obtained with the influenza virus fusion peptide which has been shown to be only slightly oblique to the membrane surface (*51*).

Oligomerization of the Fusion Peptides in Solution and in Their Membrane-Bound State. To test whether the wild type and its two mutants have similar oligomerization states in aqueous solution and in membranes, we used fluorescence spectroscopy. Since the fluorescence of rhodamine is quenched when several molecules are in close proximity, a dequenching of fluorescence should occur when an aggregated rhodamine-labeled peptide dissociates, a process that can take place when the peptide is cleaved by a proteolytic enzyme. It should be noted that rhodamine fluorescence is only slightly influenced by changes in its environment; therefore, most of the changes in the rhodamine fluorescence can be attributed to the changes in peptide aggregation. Figure 11A shows that the fluorescence of 0.1 μM Rho-WT is significantly lower than that of F11V and F11G (lanes 1). However, the fluorescence of all three peptides increases with time (lanes 2 after 15 min, and lanes 3 after 2 h) and reaches the same value upon the addition of proteinase K (0.062 mg/mL final concentration). The enzyme degrades the peptides and therefore prevents aggregation. These data indicate that the wild-type peptide is in a higher oligomerization state in solution than both mutants.

The difference between the oligomerization states of the peptides in membranes was investigated by measuring

Table 2: Analysis of the Secondary Structures of the Peptides in PC Multibilayers Obtained by Using FTIR Spectroscopy[a]

	FTIR (in dry PC multibilayers)[b,c]			FTIR (in wet PC multibilayers)[b,c]			
peptide	center of peak (area in %)			center of peak (area in %)			
wild-type	1622 (46)	1658 (25)	1674 (12)	1621 (55)	1646 (14)	1658 (5)	1674 (6)
F11V	1624 (49)	1658 (28)	1674 (10)	1623 (48)	1646 (18)	1657 (8)	1674 (23)
F11G	1626 (54)	1658 (21)	1674 (12)	1625 (50)	1644 (14)	1658 (10)	1674 (20)

[a] Center of major peaks (cm^{-1}) and calculated peak area are given. [b] A 1:50 peptide:lipid mass ratio was used. [c] The amide I frequencies characteristic of the various secondary structure elements were taken from ref *57*.

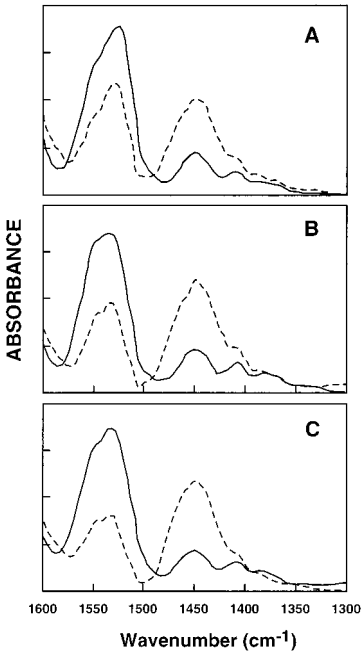

FIGURE 9: Attenuated total reflectance−Fourier transform infrared (ATR−FTIR) spectra of the amide II region of the peptides in PC multibilayers before (—) and after (- - -) wetting with D_2O for 15 min: (A) wild type, (B) F11V, and (C) F11G. The samples were prepared as described in the legend of Figure 8.

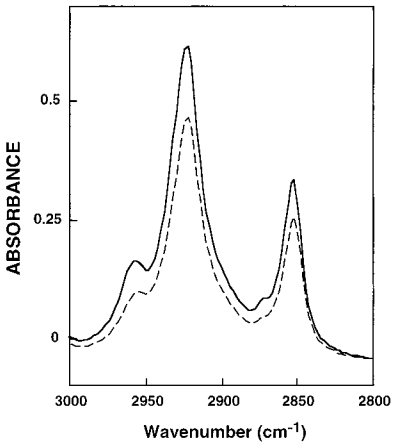

FIGURE 10: ATR dichroism spectra of parallel and perpendicular polarized ATR−FTIR absorbance spectra between 3000 and 2800 cm^{-1} for the lipid CH_2 symmetric and antisymmetric vibration of PC multibilayers. The top line is for the perpendicular component of polarized incident light, and the bottom line is for the parallel component.

peptide fluorescence in the presence of vesicles and examining the size of these peptides on a SDS−PAGE gel. Rhodamine-labeled peptides at equal concentrations were added to equal amounts of phospholipid membranes. Figure 11B shows the level of rhodamine fluorescence of the three peptides (0.1 μM) after the addition of PC SUV (lanes 1), followed by addition of proteinase K (0.062 mg/mL final concentration) (lanes 2). Similar results were obtained with PS/PC and POPG and therefore are not shown. The fluorescence of Rho-WT and that of Rho-F11V are similar and lower than that of Rho-F11G. However, the fluorescence of all three peptides reaches the same value upon addition of the enzyme. These results indicate that wild-type and

Table 3: ATR Dichroic Analysis of Lipid Orientation in Multibilayers

	dry film		hydrated with D_2O	
sample[a]	R of $\nu_{antisym}$ (~2853 cm^{-1})	f	R of $\nu_{antisym}$ (~2853 cm^{-1})	f
PC alone	1.22	0.25	1.28	0.21
PC and wild type	1.32	0.18	1.40	0.14
PC and F11V	1.36	0.16	1.43	0.12
PC and F11G	1.30	0.20	1.40	0.14

[a] Lipid:peptide molar ratios of 50:1.

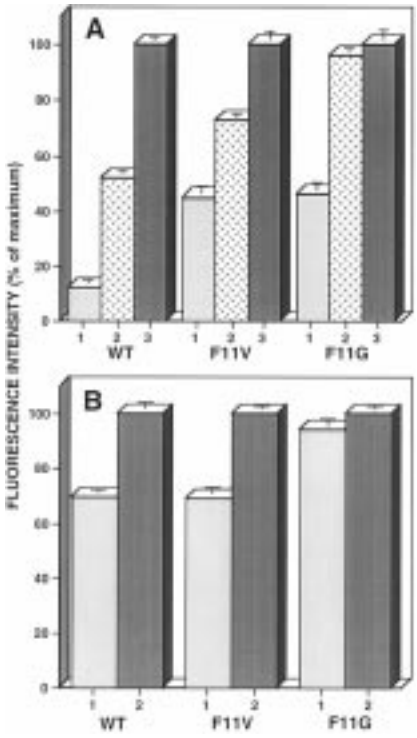

FIGURE 11: Detection of oligomerization of the peptides in aqueous solution (A) and in PC (B) SUV. (A) Rho-labeled-peptides (0.1 μM) in PBS (lanes 1) and 15 min after digestion with proteinase K (62 μg/mL) (lanes 2) and 2 h after digestion with proteinase K (lanes 3). (B) Rho-labeled peptides (0.1 μM) in PC SUV (lanes 1) and after digestion with proteinase K (62 μg/mL) (lanes 2). The excitation wavelength was set at 530 nm, and the emission was measured at 580 nm.

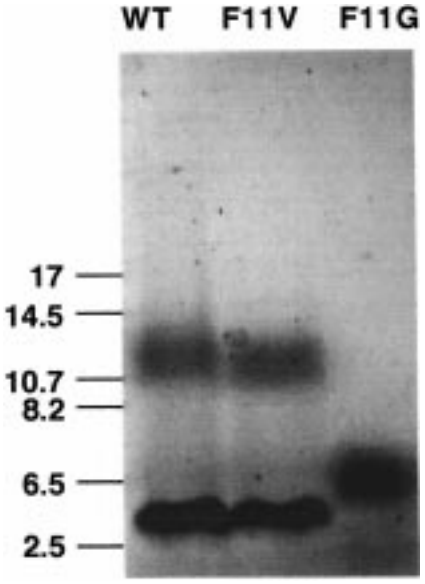

FIGURE 12: Aggregation states of the peptides determined by Tricine SDS−PAGE. The molecular masses of the the wild type, F11V, and F11G are 3264, 3216, and 3174 Da, respectively.

F11V peptides are in a similar aggregation state in the membrane which is higher than that of F11G.

The state of aggregation of peptides was also determined in SDS, which represents a membrane mimetic environment (*63*, *64*). Here, SDS−PAGE revealed (Figure 12) that the wild-type and F11V peptides have similar oligomerization states, presumably trimers or tetramers, which are higher than that observed for F11G that forms only dimers.

DISCUSSION

In this study, we examine the effect of nonpolar substitutions of the highly conserved Phe at position 11 on the fusogenic activity of the HIV-1 fusion peptide, by mimicking the previously studied F11V mutation in the intact HIV-1 fusion protein (*16*) and the F11G mutation introduced in this study (Figure 1). As in the case of the whole protein, both mutants are less active than the wild-type fusion peptide (Figures 2 and 3). These data suggest, therefore, that the properties of membrane interaction which are discussed in the following paragraphs might also play a role in virus−cell fusion. An important part in this study is the finding that the structure and function of the wild-type and the mutant peptides are not affected dramatically by the charge of the phospholipid headgroups. The wild-type peptide can promote efficiently fusion of both zwitterionic and negatively charged phospholipids without a need for secondary ions which promote vesicle aggregation. The fusion peptides studied here contain 10 additional C-terminal amino acids in addition to the predicted fusion peptide domain. Earlier studies with the fusion peptide domain alone (the 23 N-terminal amino acids) of HIV-1 showed they can promote fusion of negatively charged (PG) but not zwitterionic (PC) vesicles (*28*, *35*) unless they contain PE (*37*, *65*). PE is known for its ability to form nonbilayer structures and to enhance the fusion process (*66*). Furthermore, fusion of negatively charged membranes could be observed only in the presence of secondary cations such as Ca^{2+} or Mg^{2+} which cause vesicle aggregation, a necessary step prior to the actual fusion event (*35*). Our data suggest, therefore, that the C-terminal domain following the fusion peptide assists in membrane fusion probably by stabilizing the correct secondary structure and oligomerization state, and therefore, the elongated 33-mer represents better the fusogenic domain of gp41.

Membrane fusion is thought to involve three major steps: vesicle aggregation, membrane destabilization, and merging of the two lipid bilayers (*38*, *67*, *68*). It should be noted that in the case of the intact fusion protein intermembrane contact is not necessarily mediated by the fusion peptide, unlike in the case of intervesicle contact. Wild-type and F11V mutant peptides can induce lipid mixing of both zwitterionic and negatively charged membranes, but F11V has significantly reduced activity which is less than 50% of that of the wild type (Figures 2 and 3). F11G is not active on PC and PC/PS membranes and only slightly active on POPG. The lower fusogenic activity of F11V and F11G compared to that of the wild type is probably not associated with vesicle aggregation because (1) both the wild type and F11V have the same potency in inducing vesicle aggregation (Figure 4A) and (2) preaggregation of the peptides with Mg^{2+} caused a less than 2-fold increase in their activity, and the order of activities remained the same with or without Mg^{2+} (Figure 4B). The inability of F11G to induce membrane fusion is also not associated with vesicle aggregation since this mutant can cause vesicle aggregation, albeit with a potency of ~30% of that of the wild type (Figure 4A).

The difference between the fusogenic activity of wild-type and F11V peptides does not seem to be due to a difference in their capacity to bind vesicles, since the binding curves of both are similar and they saturate at similar lipid:peptide molar ratios (Figure 6). The binding curve of F11G saturates at higher lipid:peptide molar ratios which suggests a lower affinity for the membranes. However, this difference is not expected to affect dramatically its fusogenic activity. It is, therefore, reasonable to assume that the reduction in the fusogenic activity of F11V and the loss of activity in F11G are correlated with the last step of the fusion event, namely, merging of the two lipid bilayers.

Studies with shorter versions of fusion peptides which did not include the C-terminal domain proposed that a partial β-sheet structure is necessary for a fusion peptide to be active (*33*, *35*). Here we used FTIR spectroscopy and could not find a significant difference between the structure of the three peptides which can explain the drastic changes in their activities (Figures 8 and 9 and Table 2). An increased rate of proton exchange was detected for the mutant peptides as compared to the wild type, suggesting that the mutations destabilize the secondary structure of the fusion peptide in membranes. This may be due to the location of three nearby glycines, at positions 11, 13, and 16 which probably disrupt partially the α-helix structure. It should be noted that in other cases glycine could be accommodated as readily as alanine into a hydrophobic α-helix in a membrane (*69*). Differences in secondary structures have not been sufficient to explain differences in the activity of fusion peptides in other studies (*20*, *70*).

A basic characteristic of the fusion peptide is the extent of its penetration into the lipid bilayer and its orientation in the membrane-bound state. NBD blue shifts reveal that the N-termini of all the peptides penetrate into the hydrophobic core of the membrane with the extent of penetration of F11G being slightly less than those of the wild type and F11V

(Figure 5). Furthermore, there is not a major difference between the wild type and the two mutants in their ability to perturb the lipid order as seen in the ATR−FTIR experiments (Table 3). All of them have a small effect on the acyl chain order, supporting the suggestion of an oblique orientation in the membrane-bound state (*30*, *71*, *72*). Further support for this orientation comes from the findings that the peptides undergo complete proteolytic cleavage when bound to membranes (Figure 7) which is different from membrane-inserting peptides which are protected from cleavage (*60*).

The current model of the fusion process suggests an intermediate, a fusion pore, as a complex combining few protein molecules (*73*−*75*). In line with this model, several reports have emphasized the functional importance of the oligomeric state of the HIV-1 gp41 envelope glycoprotein. However, attempts to define its oligomeric state have yielded conflicting results. Some reports indicated that the gp41 is a tetramer in its membrane-bound state (*76*−*78*). On the other hand, other reports based on structural studies in the absence of membranes revealed that it forms trimers (*79*−*83*). In the nonfusogenic form of gp41, the fusion peptide is buried; thus, it is probably not responsible for the oligomerization of the protein. However, once the envelope glycoproteins are recruited to form a fusion complex, the exposed fusion peptides could participate in the oligomerization of the Env, shown by the ability of the isolated fusion peptides to self-associate. Here we show that fluorescently labeled wild-type, F11V, and F11G peptides are able to self-associate within phospholipid vesicles (Figures 11 and 12). The extents of oligomerization of the wild type and F11V were found to be similar, while the ability of F11G to self-associate was reduced. The inability of F11G to oligomerize properly in the membrane may be correlated with its loss of activity. Self-association of the fusion peptide of Sendai virus was also observed in PC/PS vesicles (*26*). The lower extent of aggregation of F11G in the membrane may relate to its slightly lower α-helical content, and suggests that the FLG motif has a role in the assembly of the fusion peptides in the membrane. It is reasonable to speculate that the α-helical:*β*-strand ratio plays a special role in the proper assembly of the fusion peptides as has been suggested also for the hemagglutinin fusion peptide (*24*).

It should be noted that many features of the intact virus are not present in the simple system of a peptide segment of a viral fusion protein. Unlike the intact virus, the fusogenic peptides do not bind to specific receptors on the membrane. Furthermore, there clearly are also regions outside of the fuogenic domains whose mutation can destroy the fusoginic capacity of the intact virus. For example, mutations in the heptad repeats of the measles virus fusion protein (*84*) and the gp41 of HIV (*85*) severely affected their fusion activities which further indicated the involvement of these heptad repeats in the fusion process. However, the correlation between the ability of mutant peptides to interact with membranes and the cell−cell fusion activity of the intact mutant proteins shown first in a study with planar bilayers (*86*) and then with monolayers (*87*), together with the correlation found in this study and others (*26*, *31*, *33*), supports their use in model systems. The problem of the relationship of synthetic peptides and entire viral fuogenic proteins has been discussed also by others (*86*, *88*).

Table 4: Summary of the Different Physicochemical Properties of the Peptides

	wild type	F11V	F11G
liposome fusion	+++	++	−/+
insertion into membranes	+	+	+
membrane binding	++	++	++
susceptibility to proteinase K digestion in the membrane-bound state	++	++	++
secondary structure	mainly *β*-sheet	mainly *β*-sheet	mainly *β*-sheet
self-assembly in solution	+++	++	+
self-assembly in SDS	tetramers	tetramers	dimers
self-assembly in membranes	++	++	+
effect on lipid order	+	+	+
induction of vesicle aggregation	++	++	+

In conclusion, compared with data obtained by others with short versions of the fusion peptide, we found an important role for the 10-amino acid domain following the fusion peptide region in mediating membrane fusion. The similarities and distinctions between the physicochemical properties of the wild type, F11V, and F11G are shown in Table 4. The data do not support a role for a specific structure as a predominant requirement for a peptide to induce membrane fusion, but rather a combination of several physicochemical properties. We observed differences in membrane affinity, stability of α-helical structure, and oligomerization in solution and membrane, which correlate with a decrease in the overall fusogenecity of these mutants in the context of the full-lengh evelope protein. While the synthetic peptides only partly mimic the properties of the complex viral protein, the differences in the physicochemical properties of the isolated fusion peptides and the ability of this region to induce vesicle fusion support the use of a model studies for further understanding of the fusion process.

ACKNOWLEDGMENT

We thank Dr. Y. Marikovsky for his help in visualization of the phospholipid vesicles using electron microscopy.

REFERENCES

1. Veronese, F. D., DeVico, A. L., Copeland, T. D., Oroszlan, S., Gallo, R. C., and Sarngadharan, M. G. (1985) *Science 229*, 1402−1405.
2. Lasky, L. A., Nakamura, G., Smith, D. H., Fennie, C., Shimasaki, C., Patzer, E., Berman, P., Gregory, T., and Capon, D. J. (1987) *Cell 50*, 975−985.
3. Dragic, T., Litwin, V., Allaway, G. P., Martin, S. R., Huang, Y., Nagashima, K. A., Cayanan, C., Maddon, P. J., Koup, R. A., Moore, J. P., and Paxton, W. A. (1996) *Nature 381*, 667−673.
4. Choe, H., Farzan, M., Sun, Y., Sullivan, N., Rollins, B., Ponath, P. D., Wu, L., Mackay, C. R., LaRosa, G., Newman, W., Gerard, N., Gerard, C., and Sodroski, J. (1996) *Cell 85*, 1135−1148.
5. Doranz, B. J., Rucker, J., Yi, Y., Smyth, R. J., Samson, M., Peiper, S. C., Parmentier, M., Collman, R. G., and Doms, R. W. (1996) *Cell 85*, 1149−1158.
6. Kowalski, M., Potz, J., Basiripour, L., Dorfman, T., Goh, W. C., Terwilliger, E., Dayton, A., Rosen, C., Haseltine, W., and Sodroski, J. (1987) *Science 237*, 1351−1355.
7. Trkola, A., Dragic, T., Arthos, J., Binley, J. M., Olson, W. C., Allaway, G. P., Cheng, M. C., Robinson, J., Maddon, P. J., and Moore, J. P. (1996) *Nature 384*, 184−187.

8. Lapham, C. K., Ouyang, J., Chandrasekhar, B., Nguyen, N. Y., Dimitrov, D. S., and Golding, H. (1996) *Science 274*, 602−605.
9. Moore, J. P., Trkola, A., and Dragic, T. (1997) *Curr. Opin. Immunol. 9*, 551−562.
10. Wu, L., Paxton, W. A., Kassam, N., Ruffing, N., Rottman, J. B., Sullivan, N., Choe, H., Sodroski, J., Newman, W., Koup, R. A., and Mackay, C. R. (1997) *J. Exp. Med. 185*, 1681−1691.
11. Gallaher, W. R. (1987) *Cell 50*, 327−328.
12. Durell, S. R., Martin, I., Ruysschaert, J. M., Shai, Y., and Blumenthal, R. (1997) *Mol. Membr. Biol. 14*, 97−112.
13. Freed, E. O., Myers, D. J., and Risser, R. (1990) *Proc. Natl. Acad. Sci. U.S.A. 87*, 4650−4654.
14. Bosch, M. L., Earl, P. L., Fargnoli, K., Picciafuoco, S., Giombini, F., Wong-Staal, F., and Franchini, G. (1989) *Science 244*, 694−697.
15. Horvath, C. M., and Lamb, R. A. (1992) *J. Virol. 66*, 2443−2455.
16. Delahunty, M. D., Rhee, I., Freed, E. O., and Bonifacino, J. S. (1996) *Virology 218*, 94−102.
17. Poumbourios, P., Wilson, K. A., Center, R. J., El Ahmar, W., and Kemp, B. E. (1997) *J. Virol. 71*, 2041−2049.
18. Perrin, C., Fenouillet, E., and Jones, I. M. (1998) *Virology 242*, 338−345.
19. Durrer, P., Galli, C., Hoenke, S., Corti, C., Gluck, R., Vorherr, T., and Brunner, J. (1996) *J. Biol. Chem. 271*, 13417−13421.
20. Burger, K. N., Wharton, S. A., Demel, R. A., and Verkleij, A. J. (1991) *Biochemistry 30*, 11173−11180.
21. Clague, M. J., Knutson, J. R., Blumenthal, R., and Herrmann, A. (1991) *Biochemistry 30*, 5491−5497.
22. Lear, J. D., and DeGrado, W. F. (1987) *J. Biol. Chem. 262*, 6500−6505.
23. Epand, R. M., and Epand, R. F. (1994) *Biochem. Biophys. Res. Commun. 202*, 1420−1425.
24. Gray, C., Tatulian, S. A., Wharton, W. A., and Tamm, L. K. (1996) *Biophys. J. 70*, 2275−2286.
25. Martin, I., Defrise, Q. F., Mandieau, V., Nielsen, N. M., Saermark, T., Burny, A., Brasseur, R., Ruysschaert, J. M., and Vandenbranden, M. (1991) *Biochem. Biophys. Res. Commun. 175*, 872−879.
26. Rapaport, D., and Shai, Y. (1994) *J. Biol. Chem. 269*, 15124−15131.
27. Ruiz-Arguello, M. B., Goni, F. M., Pereira, F. B., and Nieva, J. L. (1998) *J. Virol. 72*, 1775−1781.
28. Rafalski, M., Lear, J. D., and DeGrado, W. F. (1990) *Biochemistry 29*, 7917−7922.
29. Slepushkin, V. A., Melikyan, G. B., Sidorova, M. S., Chumakov, V. M., Andreev, S. M., Manulyan, R. A., and Karamov, E. V. (1990) *Biochem. Biophys. Res. Commun. 172*, 952−957.
30. Martin, I., Schaal, H., Scheid, A., and Ruysschaert, J. M. (1996) *J. Virol. 70*, 298−304.
31. Kliger, Y., Aharoni, A., Rapaport, D., Jones, P., Blumenthal, R., and Shai, Y. (1997) *J. Biol. Chem. 272*, 13496−13505.
32. Pritsker, M., Jones, P., Blumenthal, R., and Shai, Y. (1998) *Proc. Natl. Acad. Sci. U.S.A. 95*, 7287−7292.
33. Pereira, F. B., Goñi, F. M., and Nieva, J. L. (1995) *FEBS Lett. 362*, 243−246.
34. Gordon, L. M., Curtain, C. C., Zhong, Y. C., Kirkpatrick, A., Mobley, P. W., and Waring, A. J. (1992) *Biochim. Biophys. Acta 1139*, 257−274.
35. Nieva, J. L., Nir, S., Muga, A., Goñi, F. M., and Wilschut, J. (1994) *Biochemistry 33*, 3201−3209.
36. Martin, I., Dubois, M. C., Defrise-Quertain, F., Saermark, T., Burny, A., Brasseur, R., and Ruysschaert, J. M. (1994) *J. Virol. 68*, 1139−1148.
37. Martin, I., Defrise-Quertain, F., Decroly, E., Vandenbranden, M., Brasseur, R., and Ruysschaert, J. M. (1993) *Biochim. Biophys. Acta 1145*, 124−133.
38. Chernomordik, L., Kozlov, M. M., and Zimmerberg, J. (1995) *J. Membr. Biol. 146*, 1−14.
39. Alexander, W. A., Moss, B., and Fuerst, T. R. (1992) *J. Virol. 66*, 2934−2942.
40. Rucker, J., Doranz, B. J., Edinger, A. L., Long, D., Berson, J. F., and Doms, R. W. (1997) *Methods Enzymol. 288*, 118−133.
41. Merrifield, R. B., Vizioli, L. D., and Boman, H. G. (1982) *Biochemistry 21*, 5020−5031.
42. Shai, Y., Bach, D., and Yanovsky, A. (1990) *J. Biol. Chem. 265*, 20202−20209.
43. Shai, Y., Hadari, Y. R., and Finkels, A. (1991) *J. Biol. Chem. 266*, 22346−22354.
44. Rapaport, D., and Shai, Y. (1991) *J. Biol. Chem. 266*, 23769−23775.
45. Rapaport, D., and Shai, Y. (1992) *J. Biol. Chem. 267*, 6502−6509.
46. Olson, F., Hunt, C. A., Szoka, F. C., Vail, W. J., and Papahadjopoulos, D. (1979) *Biochim. Biophys. Acta 557*, 9−23.
47. Struck, D. K., Hoekstra, D., and Pagano, R. E. (1981) *Biochemistry 20*, 4093−4099.
48. Rajarathnam, K., Hochman, J., Schindler, M., and Ferguson, M. S. (1989) *Biochemistry 28*, 3168−3176.
49. Gazit, E., Miller, I. R., Biggin, P. C., Sansom, M. S. P., and Shai, Y. (1996) *J. Mol. Biol. 258*, 860−870.
50. Harrick, N. J. (1967) *Internal Reflection Spectroscopy*, Interscience, New York.
51. Ishiguro, R., Kimura, N., and Takahashi, S. (1993) *Biochemistry 32*, 9792−9797.
52. Schägger, H., and Jagow, G. V. (1987) *Anal. Biochem. 166*, 368−379.
53. Nussbaum, O., Broder, C. C., and Berger, E. A. (1994) *J. Virol. 68*, 5411−5422.
54. Wilschut, J., Düzgünes, N., and Papahadjopoulos, D. (1981) *Biochemistry 20*, 3126−3133.
55. Nir, S., Bentz, J., Wilschut, J., and Duzgunes, N. (1983) *Prog. Surf. Sci. 13*, 1−124.
56. Duzgunes, N., Allen, T. M., Fedor, J., and Papahadjopoulos, D. (1987) *Biochemistry 26*, 8435−8442.
57. Pouny, Y., and Shai, Y. (1992) *Biochemistry 31*, 9482−9490.
58. Schwarz, G., Gerke, H., Rizzo, V., and Stankowski, S. (1987) *Biophys. J. 52*, 685−692.
59. Pouny, Y., Rapaport, D., Mor, A., Nicolas, P., and Shai, Y. (1992) *Biochemistry 31*, 12416−12423.
60. Gazit, E., and Shai, Y. (1993) *Biochemistry 32*, 3429−3436.
61. Jackson, M., and Mantsch, H. H. (1995) *Crit. Rev. Biochem. Mol. Biol. 30*, 95−120.
62. Cameron, D. G., Casal, H. L., Gudgin, E. F., and Mantsch, H. H. (1980) *Biochim. Biophys. Acta 596*, 463−467.
63. Lemmon, M. A., Flanagan, J. M., Hunt, J. F., Adair, B. D., Bormann, B. J., Dempsey, C. E., and Engelman, D. M. (1992) *J. Biol. Chem. 267*, 7683−7689.
64. Simmerman, H. K. B., Kobayashi, Y. M., Autry, J. M., and Jones, L. R. (1996) *J. Biol. Chem. 271*, 5941−5946.
65. Pereira, F. B., Goni, F. M., Muga, A., and Nieva, J. L. (1997) *Biophys. J. 73*, 1977−1986.
66. Chernomordik, L. V., and Zimmerberg, J. (1995) *Curr. Opin. Struct. Biol. 5*, 541−547.
67. Nir, S., Bentz, J., and Wilschut, J. (1980) *Biochemistry 19*, 6030−6036.
68. Blumenthal, R. (1987) *Curr. Top. Membr. Transp. 29*, 203−254.
69. Li, S. C., and Deber, C. M. (1992) *FEBS Lett. 311*, 217−220.
70. Rapaport, D., Hague, G. R., Pouny, Y., and Shai, Y. (1993) *Biochemistry 32*, 3291−3297.
71. Shai, Y. (1995) *Trends Biochem. Sci. 20*, 460−464.
72. Brasseur, R., Pillot, T., Lins, L., Vandekerckhove, J., and Rosseneu, M. (1997) *Trends Biochem. Sci. 22*, 147−187.
73. White, J. M. (1992) *Science 258*, 917−924.
74. Zimmerberg, J., Vogel, S. S., and Chernomordik, L. V. (1993) *Annu. Rev. Biophys. Biomol. Struct. 22*, 433−466.
75. Lindau, M., and Almers, W. (1995) *Curr. Opin. Cell Biol. 7*, 509−517.
76. Earl, P. L., Doms, R. W., and Moss, B. (1990) *Proc. Natl. Acad. Sci. U.S.A. 87*, 648−652.
77. Pinter, A., Honnen, W. J., Tilley, S. A., Bona, C., Zaghouani, H., Gorny, M. K., and Zolla, P. S. (1989) *J. Virol. 63*, 2674−2679.

78. Schawaller, M., Smith, G. E., Skehel, J. J., and Wiley, D. C. (1989) *Virology 172*, 367−369.
79. Lu, M., Blacklow, S. C., and Kim, P. S. (1995) *Nat. Struct. Biol. 2*, 1075−1082.
80. Weiss, C. D., Levy, J. A., and White, J. M. (1990) *J. Virol. 64*, 5674−5677.
81. Weissenhorn, W., Wharton, S. A., Calder, L. J., Earl, P. L., Moss, B., Aliprandis, E., Skehel, J. J., and Wiley, D. C. (1996) *EMBO J. 15*, 1507−1514.
82. Weissenhorn, W., Dessen, A., Harrison, S. C., Skehel, J. J., and Wiley, D. C. (1997) *Nature 387*, 426−430.
83. Chan, D. C., Fass, D., Berger, J. M., and Kim, P. S. (1997) *Cell 89*, 263−273.
84. Buckland, R., Malvoisin, E., Beauverger, P., and Wild, F. (1992) *J. Gen. Virol. 73*, 1703−1707.
85. Chen, S. S., Lee, C. N., Lee, W. R., McIntosh, K., and Lee, T. H. (1993) *J. Virol. 67*, 3615−3619.
86. Duzgunes, N., and Gambale, F. (1988) *FEBS Lett. 227*, 110−114.
87. Burger, K. N., Wharton, S. A., Demel, R. A., and Verkleij, A. J. (1991) *Biochim. Biophys. Acta 1065*, 121−129.
88. Epand, R. M., Cheetham, J. J., Epand, R. F., Yeagle, P. L., Richardson, C. D., Rockwell, A., and Degrado, W. F. (1992) *Biopolymers 32*, 309−314.

BI990232E